4 Microwave Photoconductivity due to Intra-Landau-Level Transitions

Until recently, the study of two-dimensional electron systems under microwave irradiation was limited mostly to the magnetic field range where the microwave frequency ω exceeds the cyclotron frequency ω_c and microwave-induced *inter*-Landau level transitions are the relevant process. Very recently, a closely related effect was discovered by Dorozhkin *et al.* [39] and Mani [40] in ultra-high mobility systems for the case when the microwave frequency ω is *smaller* than the cyclotron frequency ω_c. The microwave irradiation is then unable to induce *inter*-LL transitions (since the absorption of a microwave photon is unable to promote an electron to a higher Landau level) and can only give rise to *intra*-LL transitions. According to Dorozhkin and co-workers, a considerable reduction of the diagonal conductivity is observed upon irradiation with microwaves of frequency $\omega \ll \omega_c$. To date, there is, however, no evidence for zero resistance states in this regime.

In this chapter, we first review the above experiments on the photoconductivity in the *intra*-LL-regime (Section 4.1). Motivated by these experiments, we study the microwave-induced photoconductivity of a two-dimensional electron gas arising from intra-Landau-level transitions within a model where the electrons are subject to a unidirectional periodic potential in addition to a weaker impurity potential. This model is presented in Section 4.2. Section 4.3 is devoted to the microscopic mechanisms leading to the photocurrent. In Section 4.4, we calculate the dark conductivity for the case where the dc current is applied parallel to the direction of the additional modulation and for the case where its direction is perpendicular to that of the modulation. In Section 4.5, we calculate the photoconductivities for both orientations. As in the *inter*-LL regime, there are contributions by the displacement mechanism as well as by the distribution function mechanism. We discuss their relative magnitude and generalize to disorder types other than smooth disorder. Section 4.6 is devoted to a comparison of our results with experiment. We argue that our model is able to explain the key experimental features even though these experiments were carried out without additional modulation potential. The reason for this lies in the fact that the realistic disorder potential can be modeled by the periodic modulation if one identifies the modulation broadening of the Landau levels within our model with the actual disorder broadening. This allows us to explain the sign of the photocurrent, its dependence on magnetic field and microwave frequency as well as the microwave-induced suppression of the Shubnikov-deHaas oscillations. In Section 4.7, we briefly comment on the polarization dependence of the photoconductivity. Section 4.8 serves as a summary of our results for the *intra*-LL regime. This chapter is based on Joas *et al.* [66].

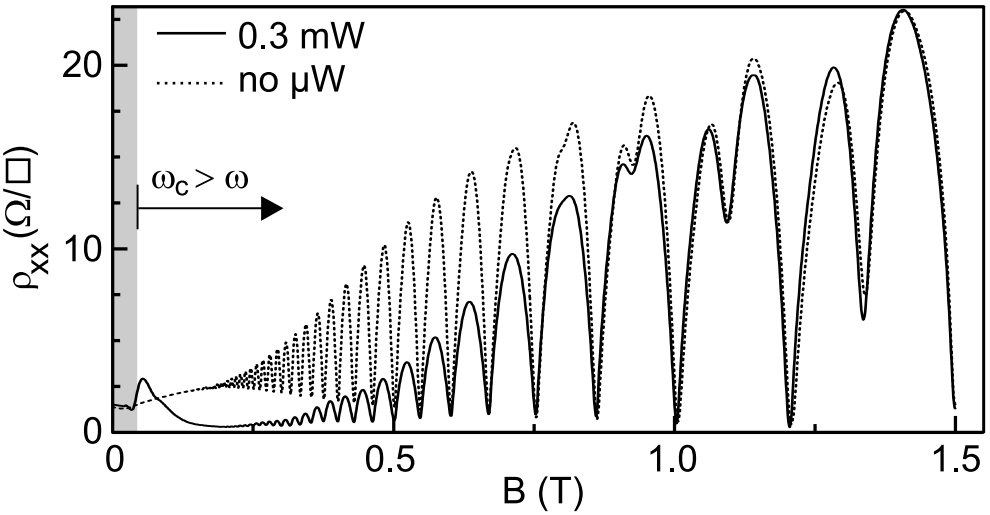

Figure 4.1: Magnetoresistivity ρ_{xx} as a function of magnetic field B in the absence of microwave irradiation (dotted curve) and under 17 GHz radiation (solid line) at a temperature of 4 K and an electronic density $n = 2.92 \times 10^{11}$ cm^{-2}. A microwave power of $P = 0.3$ mW was measured at the oscillator output. The shaded region indicates the regime $\omega > \omega_c$, whereas the unshaded region indicates the regime $\omega < \omega_c$ where intra-LL-transitions become important. This figure has been taken from Ref. [39].

4.1 Experiment

Typical experimental results for the diagonal resistivity are shown in Fig. 4.1 [39]. The dotted curve is the dark diagonal resistivity (i.e., the resistivity without microwave irradiation). As expected, ρ_{xx} exhibits the usual Shubnikov-deHaas oscillations, which are a signature of the variation of the Fermi level E_F through the Landau levels as a function of magnetic field B. The solid line, in turn, shows the result for the diagonal resistivity under irradiation with microwaves of low frequency. The average magnetoresistivity is greatly suppressed within a wide range of magnetic fields. In addition, a suppression of Shubnikov-deHaas oscillations is observed, which is most pronounced for weak magnetic fields. This result was rather unexpected since the theoretical explanations of MIRO and ZRS focus on *inter*-LL transitions (see Chapter 2). Inter-LL transitions cannot play a role in the present situation because the energy difference between the LLs greatly exceeds the energy provided by the microwave radiation, $\omega_c \gg \omega$.

The evolution of the suppression of ρ_{xx} with increasing microwave frequency is depicted in Fig. 4.2. With increasing microwave frequency, the suppression weakens and, in the inter-LL regime $\omega > \omega_c$, the expected ZRS shows up, which can be readily explained on the footing of inter-LL transitions.

In summary, the main experimental findings in the regime $\omega \ll \omega_c$ are:

- As in the regime $\omega \gg \omega_c$, the total diagonal resistivity is suppressed under microwave irradiation with respect to its dark value. The photoconductivity, defined as the irradiation-induced change in the total conductivity, is therefore negative and its amplitude increases with microwave frequency.

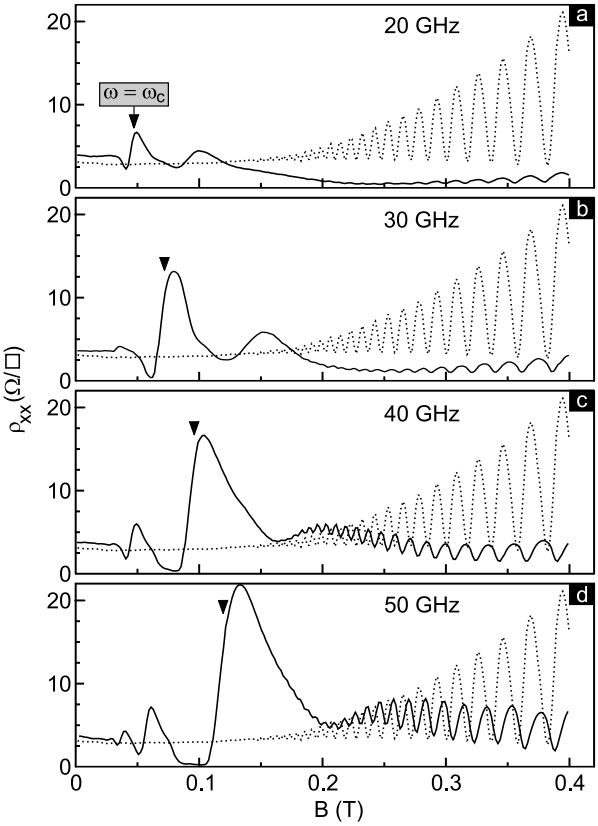

Figure 4.2: Evolution of the irradiation-induced suppression of the magnetoresistivity ρ_{xx} with increasing microwave frequency (from top to bottom) at temperature $T = 0.4$ K, density $n_s = 2.8 \times 10^{11}$ cm^{-2} and microwave output power of $P = 2$ mW. Again, the dotted curve indicates the dark magnetoresistivity, while the solid line is the magnetoresistivity under microwave irradiation. The position of the cyclotron resonance $\omega = \omega_c$ is marked by arrows. The Shubnikov-deHaas oscillations are most effectively suppressed at low frequencies. Note that the displayed range of magnetic fields is smaller than in Fig. 4.1. This figure has been taken from Ref. [39].

- Contrary to the behavior in the regime $\omega \gg \omega_c$, no ZRS are observed.
- The suppression of the diagonal conductivity is strongest for small magnetic fields. In particular, a significant suppression of Shubnikov-deHaas oscillations is observed.

4.2 Model

In order to explain these key experimental observations, a model that mimics the effect of a smooth random disorder potential via introduction of an additional periodic modulation potential turns out to be valuable. It is more accessible to analytical investigation than the full microscopic theory due to the unidirectionality of the modulation potential and its simple analytical form

(as opposed to a random potential in a realistic disorder model). A second motivation for the study of our model lies in the fact that the behavior of a 2DEG under the influence of a unidirectional periodic modulation potential (or, alternatively, more complicated modulation potentials like, e.g., a 2D modulation potential, antidot or magnetic superlattices) is interesting in itself. Its study led to the discovery of transport anisotropies [67, 68, 69, 70] and interesting commensurability oscillations known as Weiss oscillations [71, 72, 73].

4.2.1 Two-Dimensional Electron Gas in a Modulation Potential

We consider a two-dimensional electron gas (2DEG) subjected to a perpendicular magnetic field B and a unidirectional (i.e., one-dimensional), static modulation potential

$$V(\mathbf{r}) = V\cos(Qx) \tag{4.1}$$

of period $a = 2\pi/Q$, as sketched in Fig. 4.3. We further assume that the modulation potential $V(\mathbf{r})$ exceeds the residual disorder potential $U(\mathbf{r})$, whose correlator

$$W(\mathbf{r}-\mathbf{r}') = \langle U(\mathbf{r})U(\mathbf{r}')\rangle \tag{4.2}$$

falls off isotropically on the scale of the correlation length ξ. As appropriate for a high-mobility 2DEG, we assume a smooth disorder potential with correlation length

$$\xi \gg \lambda_F \quad , \tag{4.3}$$

where λ_F denotes the zero-field Fermi wavelength. The extension of our considerations to δ-correlated disorder is straightforward (see Ref. [57]). The introduction of the additional modulation potential lifts the LL degeneracy, so that a momentum transfer can be identified with a jump in real space. The photocurrent can be calculated within Fermi's golden rule, as will be shown below.

The 2DEG is irradiated by microwaves described by the electric potential

$$\phi(\mathbf{r},t) = -\frac{e}{2}\mathbf{r}(\mathbf{E}^* e^{i\omega t} + \mathbf{E}e^{-i\omega t}) = \phi_+ e^{-i\omega t} + \phi_- e^{i\omega t} \quad , \tag{4.4}$$

where

$$\phi_+ = [\phi_-]^* = -\frac{e}{2}\,\mathbf{E}\cdot\mathbf{r} \tag{4.5}$$

and $\mathbf{E}$ is the (in-plane) electric field. We consider linearly polarized microwaves whose polarization vector $\mathbf{E} = E\hat{\mathbf{x}}$ points along the x-direction, i.e. parallel to the direction of modulation. A generalization to other polarizations is easily feasible (see Section 4.7). Without loss of generality, we assume the microwave frequency ω to be positive,

$$\omega > 0 \quad . \tag{4.6}$$

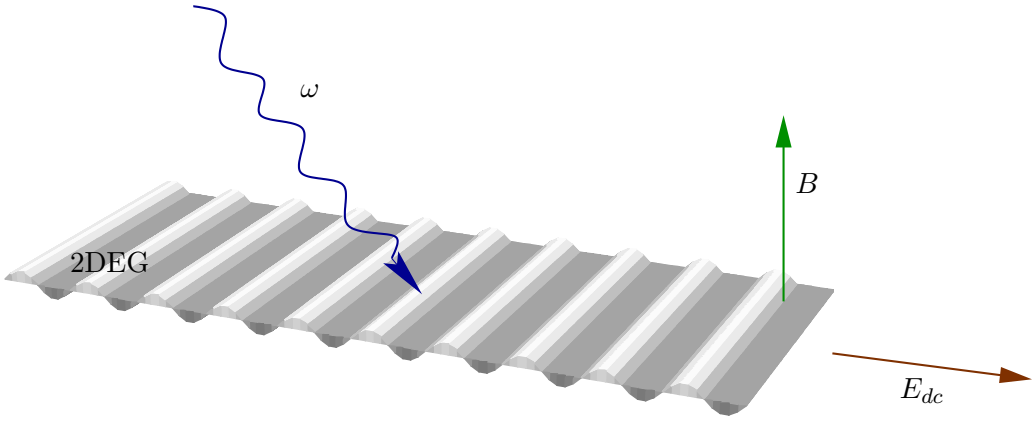

Figure 4.3: Sketch of our model of a unidirectionally modulated two-dimensional electron gas (2DEG) in a perpendicular magnetic field **B** under irradiation with microwaves of frequency ω. Shown is the so-called longitudinal case where the dc electric field E_{dc} points along the direction of modulation.

4.2.2 Electrons in High Landau Levels

At weak magnetic fields, the electrons of the 2DEG populate a large number of Landau levels, up to high LL indices n. The electronic wavefunctions in high Landau levels can be approximated by simple, asymptotic expressions as will be shown below. Before discussing the electronic states, we briefly discuss some useful relations valid in the limit of high Landau levels.

The energy of the band center of the nth LL is given by

$$E_n = \hbar\omega_c \left(n + \frac{1}{2}\right) \quad , \tag{4.7}$$

where ω_c is the cyclotron frequency, Eq. (3.5). The cyclotron radius of the nth LL, $R_c^{(n)}$, can be expressed as a function of the magnetic length $\ell_B = (\hbar/eB)^{1/2}$ as

$$R_c^{(n)} = \sqrt{2n+1}\ell_B \simeq \sqrt{2n}\ell_B \quad , \tag{4.8}$$

where the second equality is valid for large n. The ladder of Landau levels is filled up to the Fermi energy E_F. For sufficiently low temperatures $T \ll \omega_c$ and in the absence of LL mixing by disorder or modulation potential, at most one LL is partially filled. The LL index of this so-called *valence* Landau band will be denoted by $N \gg 1$. All LLs below the Nth LL are completely filled and all above are empty. In the limit of high Landau levels ($N \gg 1$), the Fermi energy can then be approximated by

$$E_F \simeq E_N = \left(N + \frac{1}{2}\right)\hbar\omega_c \simeq N\hbar\omega_c \quad . \tag{4.9}$$

The Fermi momentum $\hbar k_F = m v_F$ is related to the Fermi energy via

$$E_F = \frac{\hbar^2 k_F^2}{2m} \quad , \tag{4.10}$$

so that

$$k_F = \frac{\sqrt{2N}}{\ell_B} \quad . \tag{4.11}$$

Thus, the cyclotron radius at the Fermi level is

$$R_c = k_F \ell_B^2 \quad . \tag{4.12}$$

The above relations will be used frequently throughout this chapter.

4.2.3 Electronic States in the Absence of a Modulation Potential

We start by discussing the electronic eigenstates in the absence of disorder ($U = 0$) and microwaves ($\phi = 0$), i.e. in the unperturbed system, but at finite magnetic field B and finite driving dc electric field E_{dc}. In contrast to the case without dc electric field, angular momentum is not conserved so that the commonly used symmetric gauge $\mathbf{A} = B(-y/2, x/2)$ is inappropriate. Without modulation potential, the Landau level states $|nk\rangle$ (k denotes the momentum in y-direction) can be calculated in the Landau gauge

$$\mathbf{A} = B(0, x, 0) \quad . \tag{4.13}$$

In this gauge, the Hamiltonian for our system is

$$H = \frac{1}{2m}\left[p_x^2 + (p_y - eBx)^2\right] - eE_{dc}x \quad , \tag{4.14}$$

where p_x, p_y are the momentum components, e is the electronic charge and m the electronic mass. By using a separation ansatz for the x- and y-components of the wavefunction, one finds that in the y-direction, the eigenstates are plane waves $\exp(iky)/L_y^{1/2}$ and can be labeled by the momentum k in the y-direction. Using periodic boundary conditions in the y-direction, the allowed k values are integer multiples of $\pm 2\pi/L_y$, where L_y is the width of our system. Introducing a guiding center coordinate

$$X = k\ell_B^2 + \frac{eE_{dc}m\ell_B^4}{\hbar^2} \quad , \tag{4.15}$$

the Schrödinger equation for the x-component of the wavefunction reads

$$\left[\frac{p_x^2}{2m} + \frac{m\omega_c^2}{2}(x - X)^2\right]\psi(x) = \left[E + eE_{dc}X - \frac{m}{2}\left(\frac{E_{dc}}{B}\right)^2\right]\psi(x) \quad , \tag{4.16}$$

which is simply the equation of a harmonic oscillator whose potential is centered at $x = X$. The x-component of the eigenfunctions in position representation is then given by

$$\psi_{nk}(x) = \left(\frac{1}{\pi}\right)^{\frac{1}{4}}\left(\frac{1}{2^n n!\ell_B}\right)^{\frac{1}{2}} e^{-\frac{(x-X)^2}{2\ell_B^2}} H_n\left(\frac{x - X}{\ell_B}\right) \quad , \tag{4.17}$$

where $H_n(x)$ are Hermite polynomials. This wavefunction is extended along an equipotential line perpendicular to the electric field and localized at $x = k\ell_B^2$.

The width of the wavefunction is of the order of $\sqrt{2n+1}\ell_B \simeq \sqrt{2n}\ell_B$. Note that the momentum in y-direction, k, enters through the linear k-dependence of the guiding center, see Eq. (4.15).

The eigenenergies of the above states are given by

$$E_{nk} = \left(n + \frac{1}{2}\right)\hbar\omega_c - eE_{dc}X + \frac{m}{2}\left(\frac{E_{dc}}{B}\right)^2 \quad . \tag{4.18}$$

The first term is the energy of the cyclotron motion, the second is the potential energy in the dc electric field and the third is the kinetic energy of the drift in y-direction with velocity E_{dc}/B. Since we are interested only in the linear response properties of our system, this drift term, which is quadratic in E_{dc}, can be safely neglected. At zero dc electric field, the eigenenergies of the states $|nk\rangle$ are degenerate with respect to k.

4.2.4 Spectrum and Matrix Elements in the Presence of the Modulation Potential

For a weak modulation potential, the Landau level states $|nk\rangle$ in the Landau gauge remain good eigenstates if the amplitude V of the periodic modulation is small compared to the LL spacing $\hbar\omega_c$. We restrict our considerations to this limit. Before proceeding to a calculation of the eigenenergy with the modulation potential, we quickly discuss important matrix elements of the LL states $|nk\rangle$ for later use.

Of general use are the matrix elements of $e^{i\mathbf{q}\cdot\mathbf{r}}$ since they appear whenever a quantity is expressed in terms of a Fourier series. They are given by ($n' \geq n$)

$$\begin{aligned}\langle n'k' \left| e^{i\mathbf{q}\cdot\mathbf{r}} \right| nk\rangle &= \delta_{k',k+q_y}\sqrt{\frac{2^{n-n'}n!}{n'!}}\exp\left[-\frac{1}{4}q^2\ell_B^2 - \frac{i}{2}q_x(k+k')\ell_B^2\right] \\ &\quad \times \left[(q_y + iq_x)\ell_B\right]^{n'-n} L_n^{n'-n}\left(\frac{q^2\ell_B^2}{2}\right) \quad . \end{aligned}\tag{4.19}$$

Here, $L_n^m(z)$ are associated Laguerre polynomials. In the limit of high Landau levels and for $n = n'$, Eq. (4.19) reduces to

$$\langle nk' \left| e^{i\mathbf{q}\cdot\mathbf{r}} \right| nk\rangle = \delta_{k',k+q_y} e^{-\frac{iq_x(k+k')\ell_B^2}{2}} J_0(qR_c^{(n)}) \quad , \tag{4.20}$$

where $R_c^{(n)}$ is the cyclotron radius of the nth LL and $J_0(z)$ the zeroth order Bessel function.

We also need the matrix elements of the microwave and disorder potentials, $\phi_\pm$ and U, respectively. In what follows, we refer to ϕ_+ as microwave absorption and to ϕ_- as microwave emission. For microwaves linearly polarized in the x-direction, the matrix elements for microwave absorption and emission are the same and are given by

$$\langle n'k'|\phi_\pm|nk\rangle = -\frac{eE}{2}k\ell_B^2\delta_{n,n'}\delta_{k,k'} + \frac{eER_c}{4}\left(\delta_{n,n'-1} + \delta_{n,n'+1}\right)\delta_{k,k'} \quad . \tag{4.21}$$

Thus, absorption or emission of microwaves either leaves the LL index unchanged or couples neighboring LLs. If n and n' differ by more than one, the matrix element evaluates to zero,

$$\langle n'k'|\phi_{\pm}|nk\rangle = 0 \qquad \text{for } |n-n'|>1. \tag{4.22}$$

By contrast, the disorder potential has nonzero matrix elements between arbitrary LLs. The disorder-averaged matrix element involves the Fourier transform $\tilde{W}(\mathbf{q})$ of the correlator, Eq. (4.2), and is given by

$$\begin{aligned} |\langle n'k'|U|nk\rangle|^2 &= \int \frac{d^2q}{(2\pi)^2}\delta_{q_y,k'-k}\frac{m!}{M!}\left(\frac{q^2\ell_B^2}{2}\right)^{|n'-n|} \\ &\quad \times\left[e^{-\frac{q^2\ell_B^2}{4}}L_m^{|n'-n|}\left(\frac{q^2\ell_B^2}{2}\right)\right]^2\tilde{W}(\mathbf{q}) \quad , \end{aligned} \tag{4.23}$$

where m and M are the minimum and maximum of n and n', respectively. In the limit of high Landau levels ($n, n' \gg 1$), Eq. (4.23) can be approximated by

$$|\langle n'k'|U|nk\rangle|^2 \simeq \int \frac{d^2q}{(2\pi)^2}\delta_{q_y,k'-k}\left[J_{|n'-n|}(qR_c)\right]^2\tilde{W}(\mathbf{q}) \quad , \tag{4.24}$$

where $J_n(z)$ is a Bessel function.

The energy of an electron in state $|nk\rangle$ in the presence of the periodic modulation potential can be determined perturbatively.[1] Starting from the unperturbed Landau states $|nk\rangle$ with unperturbed energies $\hbar\omega_c(n+1/2)$, the energy correction to first order in the modulation potential is given by

$$\langle nk\,|V|\,nk\rangle = \frac{V}{2}\langle nk\,\left|e^{iQx}+e^{-iQx}\right|\,nk\rangle \quad . \tag{4.25}$$

Using the matrix elements from Eq. (4.19), this reduces to

$$\langle nk\,|V|\,nk\rangle = V_n\cos\left(Qk\ell_B^2\right) \quad , \tag{4.26}$$

where the modulation amplitude V_n is given by

$$V_n = Ve^{-Q^2\ell_B^2/4}L_n(Q^2\ell_B^2/2) \quad . \tag{4.27}$$

The energy in the modulation potential is thus given to first order by (the superscript 0 denotes the absence of a dc electric field)

$$\epsilon_{nk}^0 \simeq \hbar\omega_c(n+\frac{1}{2}) + V_n\cos(Qk\ell_B^2) \quad , \tag{4.28}$$

The additional term $V_n\cos(Qk\ell_B^2)$, which stems from the presence of the modulation potential, lifts the degeneracy with respect to k present in the modulation-free case. For large LL index n, we find that, asymptotically, Eq. (4.27) assumes the form

$$V_n \simeq VJ_0(QR_c) \quad . \tag{4.29}$$

If an additional electric field is present, the energy shifts to

$$\epsilon_{nk} = \epsilon_{nk}^0 - eE_{dc}k\ell_B^2 \quad . \tag{4.30}$$

[1] Since the electric field leads only to additive potential and drift terms in the electronic energy, we restrict the perturbative calculation of the electronic energies to the case $E_{dc}=0$ and generalize to finite dc field in the end.

4.2.5 Density of States in the Modulation Potential

At zero magnetic field, the density of states in a 2D electron system is constant and (for a spin-polarized system) is given by

$$\nu_{DOS} = \frac{m}{2\pi\hbar^2} \quad . \tag{4.31}$$

The situation changes at finite magnetic fields. In the following, we calculate the density of states at finite B in the presence of a modulation potential. The density of states (per unit area) is defined as

$$\nu(\epsilon) = \lim_{\substack{L_x \to \infty \\ L_y \to \infty}} \frac{1}{L_x L_y} \sum_n \sum_k \delta\left(\epsilon - \epsilon^0_{nk}\right) \quad , \tag{4.32}$$

where $L_x L_y$ is the area of the system and ϵ^0_{nk} the energy in the periodic modulation potential from Eq. (4.28). Taking the limit $L_y \to \infty$, the sum over k (k is the momentum in y direction) is converted into an integral, so that

$$\nu(\epsilon) = \lim_{L_x \to \infty} \frac{1}{L_x} \sum_n \int \frac{dk}{2\pi} \delta\left(\epsilon - \epsilon^0_{nk}\right) \quad . \tag{4.33}$$

Writing the energy

$$\epsilon^0_{nk} = E_n + V_n \cos(Qk\ell_B^2) \tag{4.34}$$

with $E_n = \hbar\omega_c(n + 1/2)$ and noting that for a given energy ϵ the sum over n only contributes if $|\epsilon - E_n| \leq V_n$, which, in the limit $V_n \ll \hbar\omega_c$, reduces to a single term $n = N$, N being the index of the LL energy E_N which lies closest in energy to ϵ, we get

$$\nu(\epsilon) = \lim_{L_x \to \infty} \frac{1}{L_x} \int \frac{dk}{2\pi} \delta\left(\epsilon - E_N - V_N \cos\left(\frac{2\pi\ell_B^2}{a} k\right)\right) \quad , \tag{4.35}$$

where it has been used that $Q = 2\pi/a$.

Due to the finite extension of our system, we regularize the counting of states by integrating only over states localized at $-L_x/2 \leq k\ell_B^2 \leq L_x/2$ (note that $k\ell_B^2$ simply is the x-component of the guiding center position X). Then, the length L_x drops out of the expression for the density of states and we obtain

$$\nu(\epsilon) = \frac{1}{2\pi\ell_B^2} \int_{-\pi}^{\pi} \frac{dk}{2\pi} \delta\left(\epsilon - E_N - V_N \cos(k)\right) \quad . \tag{4.36}$$

Taking the prefactor of the cosine out of the delta function, this reduces to

$$\nu(\epsilon) = \frac{1}{2\pi\ell_B^2} \frac{1}{2\pi|V_N|} \int_{-\pi}^{\pi} dk\, \delta\left(\frac{\epsilon - E_N}{V_N} - \cos(k)\right) \quad . \tag{4.37}$$

Using the well-known property [74]

$$\delta(g(x)) = \sum_j \frac{\delta(x - x_j)}{|g'(x_j)|} \qquad (g(x_j) = 0;\ g'(x_j) \neq 0) \tag{4.38}$$

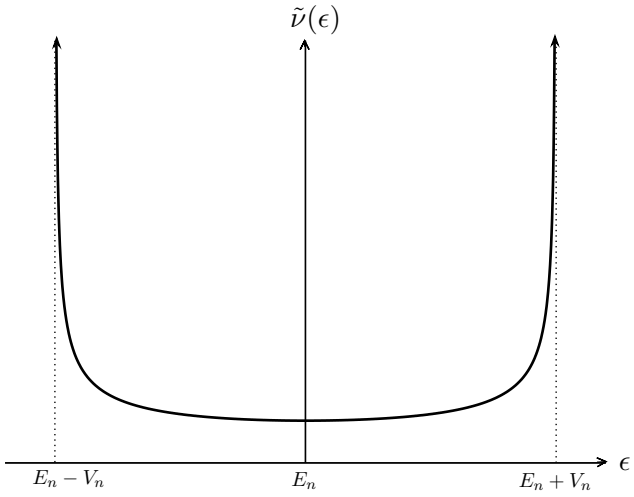

Figure 4.4: Qualitative behavior of the normalized density of states $\tilde{\nu}(\epsilon)$ for an energy ϵ satisfying $|\epsilon - E_n| \leq V_n$. The divergence at the edges of the modulation-broadened Landau band will lead to effects characteristic of the presence of a periodic modulation potential, as discussed in the main text.

of the δ function, we find

$$\nu(\epsilon) = \frac{1}{2\pi\ell_B^2} \frac{1}{2\pi|V_N|} \sum_j \int_{-\pi}^{\pi} dk \, \frac{\delta(k - k_j)}{|-\sin(k_j)|} \quad , \tag{4.39}$$

where the k_j are the zeros of

$$g(k) = \frac{\epsilon - E_N}{V_N} - \cos(k) \quad , \tag{4.40}$$

which are implicitly defined by

$$\cos(k_j) = \frac{\epsilon - E_N}{V_N} \quad . \tag{4.41}$$

This leads to

$$\sin(k_j) = \pm\sqrt{1 - \cos^2(k_j)} = \pm\sqrt{1 - \left(\frac{\epsilon - E_N}{V_N}\right)^2} \quad . \tag{4.42}$$

There are thus only two zeros of $g(k)$ in the range $-\pi \leq k \leq \pi$, whose sines are given by the above expression with positive or negative sign. Their contribution to the sum over j is the same, so that

$$\nu(\epsilon) = \frac{1}{2\pi\ell_B^2} \frac{1}{2\pi|V_N|} \frac{2}{\sqrt{1 - \left(\frac{\epsilon - E_N}{V_N}\right)^2}} \quad . \tag{4.43}$$

Defining the density of states at the band center $\epsilon = E_N$ by[2]

$$\nu^* = \nu(E_N) = \frac{1}{2\pi\ell_B^2}\frac{1}{\pi|V_N|} \tag{4.44}$$

and the normalized density of states by

$$\tilde{\nu}^*(\epsilon) = \frac{1}{\sqrt{1-\left(\frac{\epsilon-E_N}{V_N}\right)^2}} \quad , \tag{4.45}$$

the density of states in the periodic modulation potential takes the form

$$\nu(\epsilon) = \nu^*\tilde{\nu}^*(\epsilon) \quad . \tag{4.46}$$

As can be seen from Fig. 4.4, the density of states of a modulation-broadened LL diverges at the LL edges, which leads to anomalous behavior characteristic of modulation broadening as opposed to disorder broadening. This divergence is due to the flat dispersion (vanHove-type singularities) at the low- and high-energy edges of the modulation-broadened Landau bands.

4.2.6 Regimes

We are interested in the regime of intra-Landau-level transitions where

$$\omega \ll \omega_c \quad , \tag{4.47}$$

i.e. the microwave frequency lies well below the center-to-center energy difference of the Landau bands. In addition, we concentrate on the regime

$$\omega_c \gg T \gg V_N \quad . \tag{4.48}$$

Thus, the temperature smearing of the LLs is over an energy range that is large compared to their modulation broadening, but small compared to their separation. We refer to this regime as the limit of well-separated LLs.

In the limit of weak magnetic fields, i.e. of high Landau levels, we have

$$\lambda_F \ll \ell_B \ll R_c \quad , \tag{4.49}$$

where λ_F is the Fermi wavelength. We furthermore assume that the period a of the modulation potential satisfies the relation

$$\lambda_F \ll a \ll \frac{\ell_B^2}{\xi} \quad , \tag{4.50}$$

where ℓ_B^2/ξ is the real-space jump associated with a scattering event in the smooth disorder potential of correlation length ξ. The second inequality in

[2] This expression has the following simple physical interpretation: The area occupied by a LL state is $2\pi\ell_B^2$. Due to the presence of the modulation, there are only two states per period $2\pi|V_N|$ (in x-direction) of the modulation potential whose energies coincide with E_N, namely at the points where the cosine in the dispersion is zero.

relation (4.50) thus ensures that the disorder-induced jump during a scattering event is large compared to the characteristic length scale of the modulation potential.

We only provide results for spin-split LLs, assuming that the spin-splitting Zeeman energy exceeds the modulation broadening V of the LLs. This results in spin polarization of the valence LL while its counterpart (of same index but opposite spin) is either completely full or completely empty. In this way, corrections to the conductivity arise due to processes involving only one sort of spin. For spin-degenerate LLs, an additional prefactor of two has to be included in all results since twice as many electrons contribute to the current.

4.3 Mechanisms

4.3.1 General Expression for the Current

The electronic states $|nk\rangle$ are localized in x-direction at $k\ell_B^2$. The microwave field ϕ and the disorder potential U are able to induce transitions between these states. The probability amplitude of such transitions is given by the matrix elements of the corresponding T-matrix. The current in the x-direction can be expressed in terms of this T-matrix, generalizing an approach of Titeica [75].

The basic idea of the calculation of the current is sketched in Fig. 4.5. We limit our considerations to the longitudinal current j_x for a dc electric field applied parallel to the direction of modulation and will explain the necessary modifications for the transverse case when needed. The computational scheme goes as follows: We first fix an arbitrary line x_0 perpendicular to the modulation, i.e. in y-direction. Then, we count the number of scattering events which take an electron from a state k, localized at $k\ell_B^2$ to the left of our fictitious line x_0, to a state k', localized at $k'\ell_B^2$ to the right of this line, and vice versa. Due to current conservation, the results do not depend on the particular choice for x_0. We therefore average over all possible x_0. The current j_x (parallel to the direction of modulation) can then be expressed in terms of the T-matrix elements and of the electron distribution function f_{nk},

$$\begin{aligned} j_x &= \frac{2\pi e}{L_y} \int_{-\frac{L_x}{2}}^{\frac{L_x}{2}} \frac{dx_0}{L_x} \sum_{n,n'} \sum_{k<\frac{x_0}{\ell_B^2}} \sum_{k'>\frac{x_0}{\ell_B^2}} \left| \langle n'k' \left| T \right| nk \rangle \right|^2 \\ &\quad \times \quad \left[f_{nk} - f_{n'k'} \right] \delta \left(\epsilon_{nk} - \epsilon_{n'k'} \right) \quad , \end{aligned} \tag{4.51}$$

where $L_x L_y$ is the area of the system. The integral over x_0 is performed by noting that

$$\sum_{k<x_0/\ell_B^2} \sum_{k'>x_0/\ell_B^2} = \sum_k \sum_{k'} \theta(x_0 - k\ell_B^2)\theta(k'\ell_B^2 - x_0) \quad , \tag{4.52}$$

so that

$$\int_{-\frac{L_x}{2}}^{\frac{L_x}{2}} dx_0 \theta(k'\ell_B^2 - x_0)\theta(x_0 - k\ell_B^2) \longrightarrow (k' - k)\ell_B^2 \tag{4.53}$$

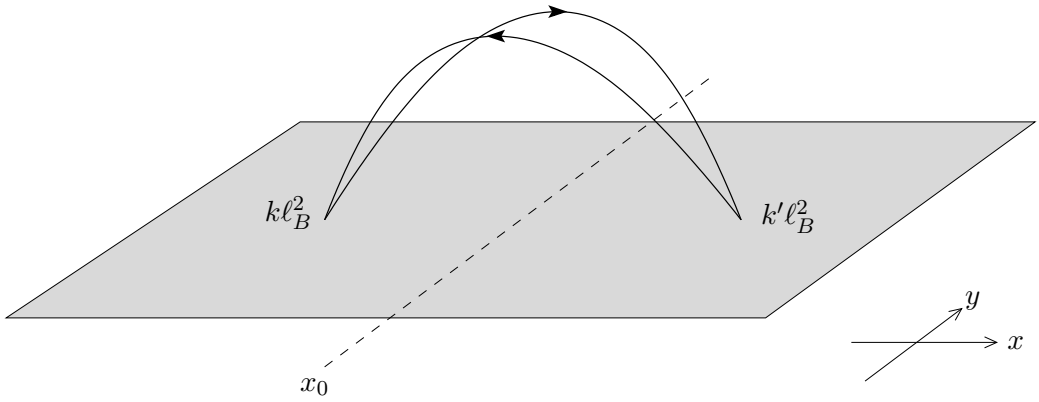

Figure 4.5: Scheme for the calculation of the current j_x as a generalization of Titeica's approach. One first defines an imaginary line at x_0, perpendicular to the modulation, and then counts the number of scattering events which take an electron from the left to the right and subtracts the number of scattering events which occur in the opposite direction. Due to current conservation, the location of the imaginary lime is irrelevant to the calculation of the current. One therefore averages over all possible x_0.

and, thereby,

$$j_x = \frac{2\pi e}{L_x L_y} \sum_{nn'} \sum_{kk'} (k'-k)\ell_B^2 \left|\langle n'k' \left|T\right| nk\rangle\right|^2 \left[f_{nk} - f_{n'k'}\right] \delta\left(\epsilon_{nk} - \epsilon_{n'k'}\right). \quad (4.54)$$

This is the general expression for the current which will be used below to compute the dark current in the absence of microwaves, and the photocurrent in the presence of microwaves.

4.3.2 Kinetic Equation

The distribution function f_{nk}, which describes the occupation of the LL eigenstates $|nk\rangle$, changes from its equilibrium value f^0_{nk} due to the presence of microwaves and disorder scattering. In addition, a realistic model has to take into account inelastic relaxation. The change in distribution function can be calculated using a kinetic approach and inelastic relaxation can be accounted for by a phenomenological relaxation time $\tau_{\rm in}$ within the relaxation time approximation. Throughout this chapter, we assume that the distribution function is uniform with respect to the spatial y-coordinate. As for the current, our considerations are valid for the longitudinal case only and will be extended to the transverse case when needed.

The distribution function f_{nk} can be obtained from the kinetic equation

$$\frac{\partial f_{nk}}{\partial t} = \left(\frac{\partial f_{nk}}{\partial t}\right)_{\rm dis} + \left(\frac{\partial f_{nk}}{\partial t}\right)_{\rm mw} - \frac{f_{\rm nk} - f^0_{\rm nk}}{\tau_{\rm in}} \quad . \quad (4.55)$$

This kinetic equation includes collision integrals for disorder scattering,

$$\left(\frac{\partial f_{nk}}{\partial t}\right)_{\rm dis} = \sum_{n'k'} 2\pi |\langle n'k'|U|nk\rangle|^2 [f_{n'k'} - f_{nk}] \delta(\epsilon_{nk} - \epsilon_{n'k'}) \quad , \quad (4.56)$$

and for disorder-assisted microwave absorption and emission,

$$\left(\frac{\partial f_{nk}}{\partial t}\right)_{\rm mw} = \sum_{n'k'}\sum_{\sigma=\pm} 2\pi|\langle n'k'|T_\sigma|nk\rangle|^2[f_{n'k'}-f_{nk}]\delta(\epsilon_{nk}-\epsilon_{n'k'}+\sigma\omega) \quad , \tag{4.57}$$

where T_σ is the contribution to the T-matrix which describes disorder-assisted microwave absorption and emission processes as will be discussed momentarily. Note that the above collision integrals involve the electron energies *including* the effects of the dc electric field

$$\epsilon_{nk} = \epsilon^0_{nk} - eE_{dc}k\ell_B^2 \quad . \tag{4.58}$$

4.3.3 T-Matrix

The full T-matrix of our system can be written as a perturbation series,

$$T = U + \phi + (U+\phi)G_0(U+\phi) + ... \quad , \tag{4.59}$$

where U is the disorder potential, ϕ the microwave potential and G_0 denotes the retarded Green's function of the unperturbed system ($U = \phi = 0$). To first order in the microwave field ϕ, there are three dominant processes: direct microwave absorption (emission) ϕ_+ (ϕ_-) and

$$T_\pm = UG_0\phi_\pm + \phi_\pm G_0 U \quad , \tag{4.60}$$

where T_+ (T_-) are referred to as disorder-assisted microwave absorption (emission). Direct microwave absorption or emission does not alter the electron momentum; it therefore does not contribute to the current. T_+ and T_-, however, do contribute to the current. These processes can be considered separately, since they contribute incoherently. The matrix elements of T_- can be shown to equal those of T_+ up to a phase.

In addition, the microwaves affect the electron distribution. The distribution function can also be expressed in terms of the T-matrix. To linear order in the microwave field, the distribution function can be written as

$$f_{nk} = f^0_{nk} + \delta f_{nk} \quad , \tag{4.61}$$

where the first-order correction δf_{nk} can be determined using the kinetic equation, Eq. (4.55). This yields

$$\begin{aligned} \delta f_{nk} &= f_{nk} - f^0_{nk} \\ &= 2\pi\tau_{\rm in}\sum_{n'k'}\sum_{\sigma=\pm}\left|\langle n'k'\left|T_\sigma\right|nk\rangle\right|^2\left[f^0_{n'k'}-f^0_{nk}\right] \\ &\qquad \times\delta\left(\epsilon^0_{nk}-\epsilon^0_{n'k'}+\sigma\omega\right) \quad . \end{aligned} \tag{4.62}$$

The general expression for the current, Eq. (4.51), can now be examined in more detail. The T-matrix enters it directly through the T-matrix elements but also indirectly via the distribution function. In what follows, we will discuss all contributions to the current up to linear order in the microwave field.

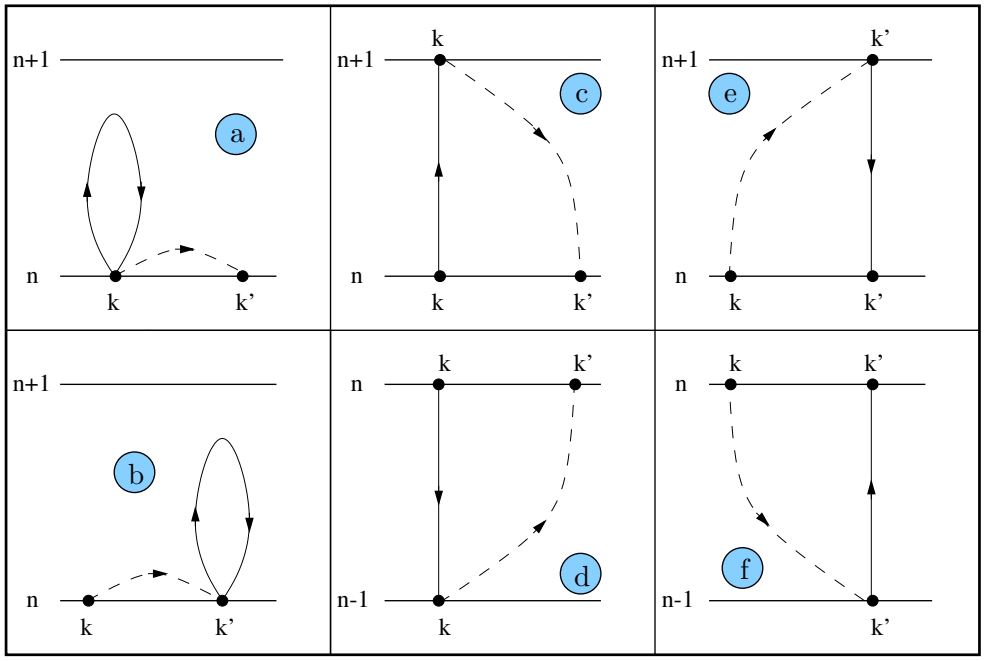

Figure 4.6: Relevant processes in the regime $\omega \ll \omega_c$. Full lines represent microwave absorption (ϕ_+) or emission (ϕ_-) and dashed lines disorder scattering (U). In processes (a) and (b), the intermediate states are in the same LL as the initial and final states. The amplitude of these processes is denoted by M_0. As shown in the main text, these processes dominate the photocurrent. For processes (c)-(f), the LL index of the intermediate states differs by one from the LL index of initial and final states. The amplitude of these processes is denoted by M_1. Their contribution can be shown to be smaller by a factor ω/ω_c than the contribution from processes (a) and (b).

4.3.4 Intra-LL-Transition Matrix Elements

In what follows, we identify the relevant microwave-induced processes by discussing the matrix elements of the corresponding contributions to the T-matrix. As mentioned above, we are interested in the case of well-separated Landau levels. In the regime $\omega \ll \omega_c$, relevant for the treatment of intra-LL transitions, only scattering processes with initial and final state in the same LL are relevant. Regardless of ω, microwaves are only able to induce transitions inside a LL or between neighboring LLs (see Eq. (4.21)). Disorder-assisted microwave absorption and emission thus proceeds via intermediate states either in the same LL (with amplitude M_0) or in neighboring LLs (with amplitude M_1), so that

$$\langle nk' \,|T_+|\, nk\rangle = M_0 + M_1 \quad . \tag{4.63}$$

These processes are depicted in Fig. 4.6 (a),(b) and (c)-(f), respectively. We find that the amplitude M_1 is smaller than M_0 by the parameter ω/ω_c. In order to demonstrate this, we first turn to the contribution M_0, which, using

Eq. (4.21), can be written as

$$\begin{aligned} M_0 &= \langle nk' \left| U \right| nk\rangle G_{0,nk}(\epsilon_{nk}+\omega)\langle nk \left| \phi_+ \right| nk\rangle \\ &\quad + \langle nk' \left| \phi_+ \right| nk'\rangle G_{0,nk'}(\epsilon_{nk})\langle nk' \left| U \right| nk\rangle \\ &= \frac{eE}{2\omega}(k'-k)\ell_B^2 \langle nk' \left| U \right| nk\rangle \quad . \end{aligned} \tag{4.64}$$

Here we used the Green function matrix elements

$$G_{0,nk}(\epsilon) = \frac{1}{\epsilon - \epsilon_{nk}} \quad , \tag{4.65}$$

so that

$$G_{0,nk}(\epsilon_{nk}+\omega) = \frac{1}{\epsilon_{nk}+\omega-\epsilon_{nk}} = \frac{1}{\omega} \tag{4.66}$$

and

$$G_{0,nk'}(\epsilon_{nk}) = \frac{1}{\epsilon_{nk}-\epsilon_{nk'}} = -\frac{1}{\omega} \quad . \tag{4.67}$$

Using Eq. (4.23), we obtain the following expression for the absolute square of the matrix element

$$|M_0|^2 \simeq \left(\frac{eE}{2\omega}\right)^2 \int \frac{d^2q}{(2\pi)^2} \delta_{q_y,k'-k} \left[q_y \ell_B^2 J_0(qR_c)\right]^2 \tilde{W}(\mathbf{q}) \quad , \tag{4.68}$$

which is valid in the limit of high Landau levels.

We now estimate the contribution M_1. The processes depicted in Fig. 4.6 (c)-(f) lead to the amplitude

$$\begin{aligned} M_1 &= \langle nk' \left| U \right| n+1k\rangle G_{0,n+1k}(\epsilon_{nk}+\omega)\langle n+1k \left| \phi_+ \right| nk\rangle \\ &\quad + \langle nk' \left| U \right| n-1k\rangle G_{0,n-1k}(\epsilon_{nk}+\omega)\langle n-1k \left| \phi_+ \right| nk\rangle \\ &\quad + \langle nk' \left| \phi_+ \right| n-1k'\rangle G_{0,n-1k'}(\epsilon_{nk})\langle n-1k' \left| U \right| nk\rangle \\ &\quad + \langle nk' \left| \phi_+ \right| n+1k'\rangle G_{0,n+1k'}(\epsilon_{nk})\langle n+1k' \left| U \right| nk\rangle \\ &= \frac{eER_c}{4}\left[\frac{\langle nk' \left| U \right| n+1k\rangle}{\omega-\omega_c} + \frac{\langle nk' \left| U \right| n-1k\rangle}{\omega+\omega_c} \right. \\ &\quad \left. - \frac{\langle n-1k' \left| U \right| nk\rangle}{\omega-\omega_c} - \frac{\langle n+1k' \left| U \right| nk\rangle}{\omega+\omega_c}\right] \quad . \end{aligned} \tag{4.69}$$

At first sight, the ratio M_1/M_0 seems to be of order $(R_c/q\ell_B^2)(\omega/\omega_c)$. For smooth disorder,

$$q \sim 1/\xi \quad , \tag{4.70}$$

so that $M_1/M_0 \sim (k_F\xi)(\omega/\omega_c)$, where $k_F\xi \gg 1$. This would imply that M_1 could actually dominate over M_0. However, this estimate turns out to be too simplistic. The reason is that for $\omega \ll \omega_c$, we can write Eq. (4.69) as

$$\begin{aligned} M_1 &= \frac{eER_c}{4\omega_c}\left\{\left[\langle n-1k' \left| U \right| nk\rangle - \langle nk' \left| U \right| n+1k\rangle\right]\right. \\ &\quad \left. + \left[\langle nk' \left| U \right| n-1k\rangle - \langle n+1k' \left| U \right| nk\rangle\right]\right\} \quad . \end{aligned} \tag{4.71}$$

We observe that the square brackets involve differences of matrix elements which differ by a uniform shift by one Landau level. It turns out that this leads to a partial cancellation which reduces our previous estimate of M_1 by $q/k_F \sim 1/k_F\xi$. As a result, we find that

$$\frac{M_1}{M_0} \sim \frac{\omega}{\omega_c} \quad , \tag{4.72}$$

as claimed above. The contribution of processes involving intermediate states outside of the valence Landau level (i.e., the topmost partially filled LL) therefore is negligible to lowest order and we may keep only the dominant contribution M_0.

4.3.5 Transport and Single-Particle Time

We now introduce two natural parameters in terms of which our results can be expressed very conveniently: transport and single-particle time. They turn out to be especially useful for the comparison of our results with results for disorder-broadened LLs.

In the presence of smooth disorder, as opposed to white-noise disorder, there are two characteristic scattering times. The first is the single-particle (or collision) time, $\tau_{\rm s}$, which is the average time between two scattering events. The second is the transport (or momentum relaxation) time, $\tau_{\rm tr}$, which encompasses a measure for the collision's effectiveness in altering the momentum of the scattered electron. If, e.g., small-angle scattering prevails, only a small fraction of momentum is lost in each individual collision. The transport time then is much larger than the single-particle time. In a 2DEG, $\tau_{\rm s}$ is much shorter than the transport time τ_{tr} due to the smooth character of the disorder potential caused by the remote donors (typically, $\tau_{tr}/\tau_s \sim 10 - 10^2$). On the other hand, in the case of delta-correlated (white noise) disorder, the scattering times coincide, $\tau_{\rm s} = \tau_{\rm tr}$. The capability of a system to prevent a current from flowing, i.e. its resistivity, depends on the transport time.

If one defines the mean free path $\ell_{\rm tr}$ as the distance an electron travels before its initial momentum is destroyed, the mean free path is simply the product of the electron velocity (typically the Fermi velocity) and the transport time,

$$\ell_{\rm tr} = v_F\, \tau_{\rm tr} \quad . \tag{4.73}$$

More quantitatively, in the case of zero magnetic field, the single particle time can be expressed in terms of the correlator of the disorder potential via ($\langle\cdot\rangle_{\rm FS}$ denotes an average over the Fermi surface)

$$\frac{1}{\tau_{\rm s}} = 2\pi \sum_{\mathbf{q}} \tilde{W}(\mathbf{q}) \langle \delta(\epsilon_k - \epsilon_{k+q})\rangle_{\rm FS} = \frac{1}{\pi v_F} \int_0^\infty dq\, \tilde{W}(\mathbf{q}) \quad , \tag{4.74}$$

where ϵ_k is the zero-field dispersion. The transport time, in turn, is given by

$$\begin{aligned} \frac{1}{\tau_{\rm tr}} &= 2\pi \sum_{\mathbf{q}} (1 - \cos\theta_{\mathbf{q}}) \tilde{W}(\mathbf{q}) \langle \delta(\epsilon_k - \epsilon_{k+q})\rangle_{\rm FS} \\ &= \frac{1}{\pi v_F} \int_0^\infty dq\, \frac{q^2}{2k_F^2} \tilde{W}(\mathbf{q}) \quad , \end{aligned} \tag{4.75}$$

where $\theta_{\mathbf{q}}$ denotes the scattering angle. These relations yield immediately that

$$\frac{\tau_{\mathrm{tr}}}{\tau_{\mathrm{s}}} \sim (k_F \xi)^2 \quad . \tag{4.76}$$

It is obvious from classical considerations that both, collision and single-particle times, change in the presence of a magnetic field that forces the electrons on cyclotron orbits. In the presence of a magnetic field, the transport and single-particle times become energy-dependent and will be denoted by $\tau^*_{\mathrm{tr}}(\epsilon)$ and $\tau^*_{\mathrm{s}}(\epsilon)$, respectively. The relation of the finite-B-field transport time to the transport time in the absence of a magnetic field is

$$\tau^*_{\mathrm{tr}}(\epsilon) = \tau_{\mathrm{tr}} \frac{\nu}{\nu^*(\epsilon)} \quad , \tag{4.77}$$

whereas for the single-particle times the relation reads

$$\tau^*_s(\epsilon) = \tau_s \frac{\nu}{\nu^*(\epsilon)} \quad . \tag{4.78}$$

Here, ν is the (constant) density of states in the absence of a magnetic field and $\nu^*(\epsilon)$ the energy-dependent density of states in the presence of a magnetic field from Eq. (4.46). The ratio of the two scattering times, Eq. (4.76), however, stays the same regardless of the presence of a magnetic field. This follows immediately from Eqs. (4.77-4.78) due to the common factor $\nu/\nu^*(\epsilon)$.

In this chapter, we assume the presence of a smooth disorder potential as suggested by the experimental scenario. There is, however, no need to restrict ourselves to this particular realization of disorder. A generalization to, e.g., white noise (delta-correlated) disorder is straightforward. Up to numerical prefactors, the results for white-noise disorder can be obtained from our results for smooth disorder by setting

$$\tau_{\mathrm{tr}} = \tau_{\mathrm{s}} \quad . \tag{4.79}$$

4.4 Dark Current

4.4.1 Longitudinal Dark Current

The dark current, i.e. the current in the absence of microwaves, can be obtained from Eq. (4.51) by inserting $T = U$. We assume that the dc electric field is sufficiently weak, so that heating effects can be ignored. Then, the electron distribution function remains in equilibrium and we can set $f_{nk} = f^0_{nk}$ in Eq. (4.51). We start by computing the longitudinal dark current, i.e. the current parallel to the direction of the static periodic modulation. Using the general expression for the current, Eq. (4.54), the longitudinal dark current is given by

$$j_x = \frac{2\pi e}{L_x L_y} \sum_{nn'} \sum_{kk'} (k' - k) \ell_B^2 \left| \langle n'k' \left| U \right| nk \rangle \right|^2 \left[f^0_{nk} - f^0_{n'k'} \right] \delta \left(\epsilon_{nk} - \epsilon_{n'k'} \right) . \tag{4.80}$$

Inserting the disorder matrix elements from Eq. (4.23) and performing the sum over k' leads to

$$\begin{aligned} j_x &= \frac{\pi e}{L_x L_y} \sum_{nk} \int \frac{d^2q}{(2\pi)^2} \Bigg\{ q_y \ell_B^2 e^{-\frac{q^2\ell_B^2}{2}} \left[L_n\left(\frac{q^2\ell_B^2}{2}\right)\right]^2 \\ &\times \tilde{W}(\mathbf{q}) \left[f^0_{nk} - f^0_{n'k'} \right] \delta\left(\epsilon^0_{nk} - \epsilon^0_{n'k+q_y} + eE_{dc} q_y \ell_B^2 \right) \Bigg\} \quad . \end{aligned} \tag{4.81}$$

Expanding to linear order in the dc electric field, this yields for the conductivity

$$\begin{aligned} \sigma_{xx} &= \frac{\pi e^2}{L_x L_y} \sum_{nk} \left(-\frac{\partial f^0_{nk}}{\partial \epsilon^0_{nk}} \right) \int \frac{d^2q}{(2\pi)^2} \Bigg\{ \left(q_y \ell_B^2\right)^2 \\ &\times e^{-\frac{q^2\ell_B^2}{2}} \left[L_n\left(\frac{q^2\ell_B^2}{2}\right)\right]^2 \tilde{W}(\mathbf{q}) \delta\left(\epsilon^0_{nk} - \epsilon^0_{n'k+q_y} \right) \Bigg\} \quad . \end{aligned} \tag{4.82}$$

The remaining integral can be computed by noting that it factorizes into two parts. The first is a separate averaging over the delta function while the second is the remainder of the integral which is cut off at large q due to the correlator of the smooth disorder. Since we are only interested in weak magnetic fields, i.e. high LLs, we can employ the semiclassical asymptotics of the Laguerre polynomials

$$e^{-\frac{q^2\ell_B^2}{4}} L_n\left(\frac{q^2\ell_B^2}{2}\right) \simeq \sqrt{\frac{2}{\pi q R_c}} \cos\left(q R_c - \frac{\pi}{4} \right) \quad . \tag{4.83}$$

In total, the dark longitudinal conductivity can be expressed in terms of an integral over energy involving the density of states

$$\sigma_{xx} = e^2 \int d\epsilon \left(-\frac{\partial f^{(0)}(\epsilon)}{\partial \epsilon} \right) \nu^*(\epsilon) \frac{R_c^2}{2\tau^*_{\mathrm{tr}}(\epsilon)} \quad . \tag{4.84}$$

This result can be interpreted as follows: The bare rate for disorder scattering is $1/\tau^*_{\mathrm{s}}$. Each scattering event is associated with a momentum transfer $1/\xi$. This momentum transfer is associated with a jump of magnitude ℓ_B^2/ξ in real space. The electron therefore diffuses in x-direction with a diffusion constant $D_{xx} \sim \left(\ell_B^2/\xi\right)^2 / \tau^*_{\mathrm{s}}$. Alternatively, this diffusion constant can be expressed in terms of the transport time as $D_{xx} = R_c^2/2\tau^*_{\mathrm{tr}}$, where the relation $\tau^*_{\mathrm{tr}}/\tau^*_{\mathrm{s}} \sim (k_F\xi)^2$ has been used. By the Einstein relation, this diffusion constant translates into the conductivity given in the integrand of Eq. (4.84). Note that, due to the singular density of states $\nu^*(\epsilon)$, the integral in Eq. (4.84) is formally logarithmically divergent. The divergence is cut off by smearing of the band edge due to disorder or (if the dc electric field is treated beyond linear order) by the applied dc electric field.

4.4.2 Transverse Dark Current

An applied dc field in y-direction leads to a nonequilibrium distribution function f_{nk} due to a drift term in y-direction that enters the kinetic equation (see also

Section 4.5.2) [57]. The drift term

$$-eE_{dc}\frac{\partial f_{nk}}{\partial k} \tag{4.85}$$

enters the right-hand side of the kinetic equation, Eq. (4.55), which then reads

$$\frac{\partial f_{nk}}{\partial t} = \left(\frac{\partial f_{nk}}{\partial t}\right)_{\rm dis} + \left(\frac{\partial f_{nk}}{\partial t}\right)_{\rm mw} - \frac{f_{\rm nk} - f^0_{\rm nk}}{\tau_{\rm in}} - eE_{dc}\frac{\partial f_{nk}}{\partial k} \quad . \tag{4.86}$$

The deviation from the equilibrium distribution function $\delta f_{nk} = f_{nk} - f^{(0)}_{nk}$ can then be calculated by linearizing the stationary kinetic equation in the applied dc electric field and neglecting inelastic processes relative to elastic disorder scattering. Then, the kinetic equation is given by

$$\begin{aligned} eE_{dc}\frac{\partial f^{(0)}_{nk}}{\partial k} &= 2\pi \int \frac{d^2q}{(2\pi)^2} e^{-q^2\ell_B^2/2}\left[L_n\left(\frac{q^2\ell_B^2}{2}\right)\right]^2 \\ &\times \tilde{W}(\mathbf{q})\left[\delta f_{nk+q_y} - \delta f_{nk}\right]\delta(\epsilon^{(0)}_{nk} - \epsilon^{(0)}_{nk+q_y}) \quad . \end{aligned} \tag{4.87}$$

As in the case of the longitudinal dark current, the transverse dark conductivity can be expressed in terms of an integral over energy involving the density of states

$$\sigma_{yy} = e^2 \int d\epsilon \left(-\frac{\partial f^{(0)}(\epsilon)}{\partial \epsilon}\right) \nu^*(\epsilon)\left[v_y(\epsilon)\right]^2 \tau_s^*(\epsilon) \quad , \tag{4.88}$$

where the drift velocity v_y is given by

$$|v_y(\epsilon)| = \left|\frac{\partial \epsilon^{(0)}_{nk}}{\partial k}\right| = \frac{1}{\pi a \nu^*(\epsilon)} \quad . \tag{4.89}$$

The interpretation of this result is based on the idea that, with respect to electron motion in the y-direction, a partially filled LL consists of a set of two "internal edge channels" per period a, which are parallel to the y-direction. In neighboring channels, the electrons flow in opposite directions, so that after a time τ_s^*, the direction of motion is randomized due to disorder scattering. The factor $D_{yy} = [v_y(\epsilon)]^2\tau_s^*$ can thus be interpreted as the corresponding diffusion constant and, by the Einstein relation, directly translates into the conductivity, Eq. (4.88).

4.5 Photocurrent

We now move on to the calculation of the photocurrent for the regime of intra-LL transitions. To lowest order, there is no current due to the microwaves (ϕ) alone since they conserve momentum as can be seen from the relevant matrix element (see Section 4.2.4). Only in second order, where terms $U\phi$ or ϕU appear in the T-matrix, the microwaves are able to induce a current via disorder-assisted photoabsorption and -emission. In the limit of high Landau levels and for well-separated LLs, the main contributions to the photocurrent

arise from disorder-assisted microwave absorption or emission processes with intermediate states inside the valence LL of index N, corresponding to the contributions

$$T_{\pm} = UG_0\phi_{\pm} + \phi_{\pm}G_0U \tag{4.90}$$

to the T-matrix.

In perturbation theory, disorder-assisted microwave absorption or emission leads to two separate contributions to the photocurrent. The first contribution is due to the displacement mechanism (DP) and the second to the distribution function mechanism (DF), both discussed briefly in Section 2.2.2.

First, disorder-assisted microwave absorption or emission changes the electron momentum from k to k', which effectively corresponds to real-space jumps in the x-direction of length $(k'-k)\ell_B^2$. Due to the applied dc electric field, these jumps occur preferentially in a fixed direction. Within the generalized approach of Titeica [75], this displacement contribution to the longitudinal photocurrent can be expressed as

$$\begin{aligned} j_x^{\mathrm{DP}} = \frac{\pi e}{L_x L_y} \sum_{\sigma=\pm} \sum_{n} \sum_{k,k'} (k'-k)\ell_B^2 \left|\langle nk' \left|T_\sigma\right| nk\rangle\right|^2 \\ \times \quad \left[f_{nk}^0 - f_{nk'}^0\right] \delta(\epsilon_{nk} - \epsilon_{nk'} + \sigma\omega) \quad . \end{aligned} \tag{4.91}$$

Here f_{nk}^0 is the equilibrium electron distribution function and

$$\epsilon_{nk} = \epsilon_{nk}^0 - eE_{dc}k\ell_B^2 \tag{4.92}$$

is the Landau level energy including the effect of the dc electric field. If one were to include a nonequilibrium distribution function in the above expression for the photocurrent, this current would be of second order in the microwave fields, which lies beyond the scope of this work.

Secondly, the microwaves change the electronic distribution function away from equilibrium. The resulting distribution function contribution to the longitudinal photocurrent is

$$\begin{aligned} j_x^{\mathrm{DF}} = \frac{\pi e}{L_x L_y} \sum_{n} \sum_{k,k'} (k'-k)\ell_B^2 \left|\langle nk' \left|U\right| nk\rangle\right|^2 \\ \times \quad \left[\delta f_{nk} - \delta f_{nk'}\right] \delta(\epsilon_{nk} - \epsilon_{nk'}) \quad , \end{aligned} \tag{4.93}$$

where

$$\delta f_{nk} = f_{nk} - f_{nk}^0 \tag{4.94}$$

is the deviation of the nonequilibrium electron distribution function f_{nk} from the equilibrium distribution f_{nk}^0 which can be obtained from the kinetic equation (see Section 4.3.2).

In what follows, we will first calculate these contributions for the longitudinal photocurrent, making use of the machinery developed in the above calculation of the dark current. Since it turns out that, in the – experimentally relevant – limit of slow inelastic relaxation,[3] the DF contribution to the longitudinal photocurrent dominates parametrically over the DP contribution to the longitudinal photocurrent, we will start by discussing the distribution function contribution.

[3] For this case, it is reasonable to expect that our results for the magnitude of the photocurrent

4.5.1 Longitudinal Photocurrent

In this section, we compute the photocurrent for dc electric fields applied along the modulation direction.

Distribution Function Mechanism

The microwave-induced change in the distribution function, as obtained from the kinetic equation (4.55), equals

$$\begin{aligned} \delta f_{Nk} &= \tau_{\rm in} \sum_{k'} \sum_{\sigma} 2\pi |\langle Nk'|T_\sigma|Nk\rangle|^2 \\ &\times \left[f^0_{Nk'} - f^0_{Nk}\right] \delta(\epsilon^0_{Nk} - \epsilon^0_{Nk'} + \sigma\omega) \quad , \end{aligned} \tag{4.95}$$

where N denotes the valence Landau level in which the Fermi energy is situated. This valence LL is the only partially filled LL, all others are either completely filled or empty. Since there is no change in the distribution function for other Landau levels than the valence LL, δf_{nk} vanishes for all other Landau levels $n \neq N$. In the considered limit $\omega_c \gg T \gg V$, the distribution function changes only weakly within the Landau level. The difference of the equilibrium distribution functions can then be approximated as

$$\begin{aligned} f^0_{nk} - f^0_{nk'} &= n_F(\epsilon_{nk}) - n_F(\epsilon_{nk'}) \\ &= n_F(\epsilon_{nk}) - n_F(\epsilon_{nk} - \sigma\omega) \\ &\simeq -\omega \frac{\partial n_F(\epsilon_{nk} + \sigma\omega)}{\partial \omega}\bigg|_{\omega=0} \quad , \end{aligned} \tag{4.96}$$

where $n_F(\epsilon)$ denotes the Fermi-Dirac distribution. Now ($\beta = 1/k_B T$),

$$\begin{aligned} \frac{\partial n_F(\epsilon_{nk} + \sigma\omega)}{\partial \omega}\bigg|_{\omega=0} &= \left[\frac{\partial}{\partial \omega}\left(\frac{1}{1+\exp\left(\beta\left(\epsilon_{nk} + \sigma\omega\right)\right)}\right)\right]\bigg|_{\omega=0} \\ &= -\sigma\beta \frac{1}{1+\exp(\beta\epsilon_{nk})}\left[1 - \frac{1}{1+\exp(\beta\epsilon_{nk})}\right] \\ &= -\sigma\beta n_F(\epsilon_{nk})\left[1 - n_F(\epsilon_{nk})\right] \quad , \end{aligned} \tag{4.97}$$

so that

$$f^0_{nk} - f^0_{nk'} = \sigma\beta\omega n_F(\epsilon_{nk})\left[1 - n_F(\epsilon_{nk})\right] \quad . \tag{4.98}$$

We assumed that $T \gg V$, so that the temperature smearing occurs over an energy range large compared to the LL width. Then, $n_F(\epsilon_{nk})$ does not depend on k. If now $n \neq N$, either $n_F(\epsilon_{nk})$ or $[1 - n_F(\epsilon_{nk})]$ is zero, so that , for $n \neq N$,

$$f^0_{nk} - f^0_{nk'} = 0 \quad (n \neq N) \quad , \tag{4.99}$$

will be parametrically identical to those obtained by calculations for disorder-broadened Landau levels, provided we identify the Landau-level broadenings due to periodic potential and disorder. Indeed, this was found to be true in earlier work on the photoconductivity due to inter-LL transitions [57]. At the same time, it is expected that the frequency dependence of the photoconductivity will be sensitive to the specific density of states of our model.

as stated above. For $n = N$, in turn, we find

$$f^0_{Nk'} - f^0_{Nk} \simeq -\sigma\beta\omega n_F(\epsilon^0_{Nk})[1 - n_F(\epsilon^0_{Nk})] \quad . \tag{4.100}$$

Noting that, in the limit $\omega_c \gg T$, to leading order $n_F(\epsilon^0_{Nk})$ is just the partial filling factor ν^*_N of the valence Landau level, we obtain the relation

$$f^0_{Nk'} - f^0_{Nk} \simeq -\sigma\beta\omega\nu^*_N(1 - \nu^*_N) \quad . \tag{4.101}$$

Thus, the change in the distribution function is maximal for half-filled (valence) Landau levels and falls off to zero for empty and completely occupied Landau levels.

Inserting the expression (4.68) for the matrix element and performing the sum over k', we obtain

$$\begin{aligned} \delta f_{Nk} &= -2\pi\tau_{\rm in}\beta\omega\nu^*_N(1-\nu^*_N)\left(\frac{eE}{2\omega}\right)^2 \sum_\sigma \sigma \int \frac{d\mathbf{q}}{(2\pi)^2}[q_y\ell_B^2 J_0(qR_c)]^2 \\ &\times \tilde{W}(\mathbf{q})\delta(\epsilon^0_{Nk} - \epsilon^0_{Nk+q_y} + \sigma\omega) \quad . \end{aligned} \tag{4.102}$$

The $\mathbf{q}$-integration is simplified significantly in the limit $\lambda_F \ll a \ll \ell_B^2/\xi$, where it factorizes into an average over the δ-function which oscillates on a q-scale of a/ℓ_B^2 and an integral over the remaining integrand. The average over the δ-function can be expressed through the Landau-level density of states, Eq. (4.46),

$$\langle\delta(\epsilon^0_{Nk} - \epsilon^0_{Nk+q_y} + \sigma\omega)\rangle_{q_y} = 2\pi\ell_B^2\nu^*(\epsilon^0_{Nk} + \sigma\omega)\theta(V - |\epsilon^0_{Nk} + \sigma\omega|) \quad . \tag{4.103}$$

The remaining integrand consists of the correlator $\tilde{W}(q)$, which falls of on the scale $1/\xi$ and the Laguerre polynomial which oscillates as a function of $q\ell_B^2$ on the scale λ_F and decays within a scale of the order of the cyclotron radius R_c. Exploiting the fact that the integrand of the remaining q-integration is cut off by the correlator $\tilde{W}(q)$ at large q, we can replace the Bessel function by its asymptotic expression for large argument from Eq. (4.83)

$$e^{-\frac{q^2\ell_B^2}{4}} L_n\left(\frac{q^2\ell_B^2}{2}\right) \simeq \sqrt{\frac{2}{\pi q R_c}}\cos\left(qR_c - \frac{\pi}{4}\right) \tag{4.104}$$

In this way, we can relate the remaining integral

$$\int_0^\infty dq q^2 \tilde{W}(q) \tag{4.105}$$

to the zero-field transport time, defined by Eq. (4.75)

$$\frac{1}{\tau_{\rm tr}} = \frac{1}{\pi v_F}\int_0^\infty dq\left(\frac{q^2}{2k_F^2}\right)\tilde{W}(q) \tag{4.106}$$

as

$$\int_0^\infty dq q^2 \tilde{W}(q) = \frac{2\pi v_F k_F^2}{\tau_{\rm tr}} \quad . \tag{4.107}$$

From Eq. (4.77), we know that

$$\frac{1}{\tau_{\rm tr}^*(\epsilon_{Nk}^0+\sigma\omega)} = \frac{1}{\tau_{\rm tr}}\frac{\nu^*(\epsilon_{Nk}^0+\sigma\omega)}{\nu} \quad , \tag{4.108}$$

where $\nu = m/(2\pi\hbar^2)$ is the constant density of states in the absence of a magnetic field. Rewriting the transport time without magnetic field in terms of the transport time with magnetic field and using Eqs. (4.102-4.103), the change in the distribution function can be expressed as

$$\begin{aligned}\delta f_{Nk} = &-\beta\omega\nu_N^*(1-\nu_N^*)\left(\frac{eER_c}{2\omega}\right)^2 \\ &\times \quad \sum_\sigma \sigma \frac{\tau_{\rm in}}{\tau_{\rm tr}^*(\epsilon_{Nk}^0+\sigma\omega)}\theta(V-|\epsilon_{Nk}^0+\sigma\omega|) \quad .\end{aligned} \tag{4.109}$$

This expression is to be inserted into Eq. (4.93).

The change in distribution function δf_{Nk} calculated above enables us to calculate the longitudinal DF photocurrent. This involves a number of arguments encountered already in the previous calculation. Expanding the average over the delta function in Eq. (4.93) to linear order in E_{dc}, the longitudinal distribution photoconductivity can be written as

$$\begin{aligned}\sigma_{xx}^{DF} &= \frac{\pi e^2}{L_x L_y}\sum_{nk}\left(-\frac{\partial\delta f_{nk}}{\partial\epsilon_{nk}^0}\right)\int\frac{d^2q}{(2\pi)^2} \\ &\times \quad \left[q_y\ell_B^2 J_0(qR_c)\right]^2\tilde{W}(\mathbf{q})2\pi\ell_B^2\nu^*(\epsilon_{nk}^0) \quad .\end{aligned} \tag{4.110}$$

Again, the asymptotic form of the Bessel function can be used, since we are interested in high LLs. In addition, we are again able to relate the remaining integral to the transport time using Eq. (4.107). Performing these steps yields

$$\sigma_{xx}^{\rm DF} = \left(e^2\frac{R_c^2}{2\tau_{\rm tr}^*}\nu^*\right)\frac{2\pi\ell_B^2}{L_xL_y}2\pi V\sum_k\left(-\frac{\partial\delta f_{Nk}}{\partial\epsilon_{Nk}^0}\right)\tilde{\nu}^*(\epsilon_{Nk}^0) \quad . \tag{4.111}$$

The remaining task consists of the evaluation of the sum over k. This is done in close analogy to the dark current, where we expressed the sum over k as an integral over energy involving the density of states. We finally obtain the result

$$\begin{aligned}\sigma_{xx}^{\rm DF} &= -2\,\beta\omega\,\nu_N^*(1-\nu_N^*)\left(e^2\frac{R_c^2}{2\tau_{\rm tr}^*}\nu^*\right)\left(\frac{eER_c}{2\omega}\right)^2\frac{\tau_{\rm in}}{\tau_{\rm tr}^*} \\ &\times\, B_1\left(\frac{\omega}{2V_N}\right) \quad ,\end{aligned} \tag{4.112}$$

where

$$B_1\left(\frac{\omega}{2V_N}\right) = -\frac{\partial}{\partial\omega}\int_{-V}^{V-\omega}d\epsilon[\tilde{\nu}^*(\epsilon)]^2\tilde{\nu}^*(\epsilon+\omega) \quad . \tag{4.113}$$

This integral is formally logarithmically divergent. However, both the presence of disorder and the dc electric field introduce an energy broadening of the LL edge, so that the divergence is cut off. The result is

$$B_1(x) = \frac{1}{16}\frac{1-2x}{(x-x^2)^{3/2}}\ln\left(\frac{V_N}{\Delta}\right) \quad , \tag{4.114}$$

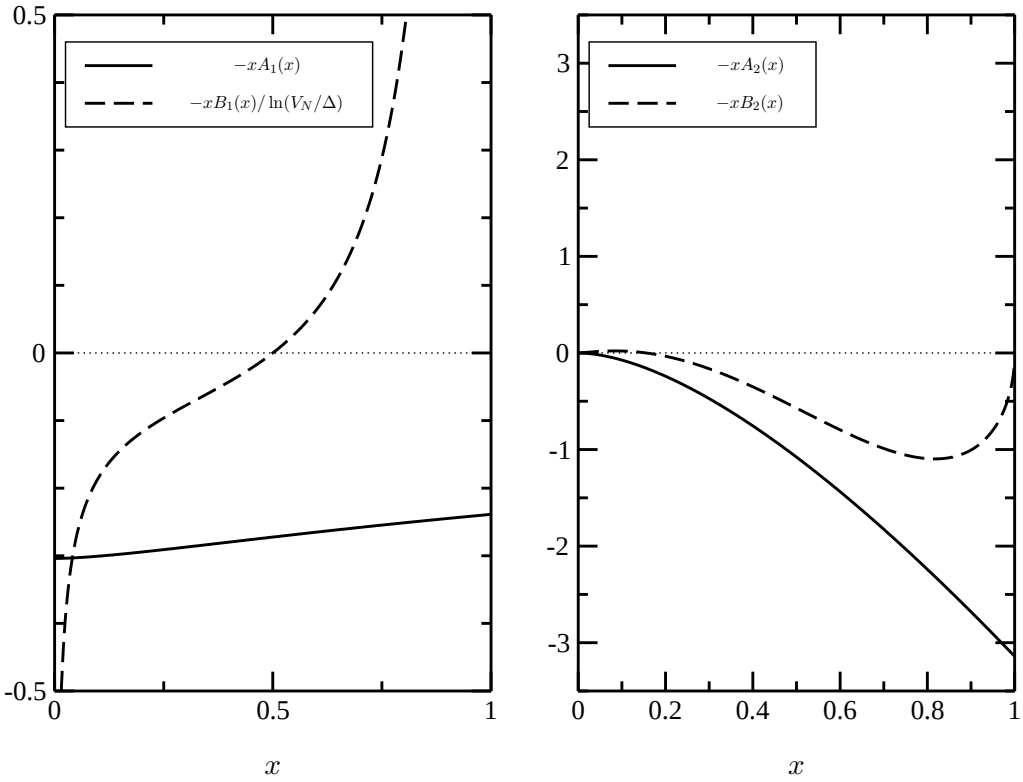

Figure 4.7: Sign and frequency dependence of the photocurrent. Left panel: functions $-xA_1(x)$(full line) and $-xB_1(x)/\ln(V_N/\Delta)$(dashed) determining the sign and frequency dependence of the displacement and distribution-function contributions to the longitudinal photoconductivity, respectively (with $x = \omega/2V_N$). Right panel: the corresponding functions $-xA_2(x)$(full line) and $-xB_2(x)$(dashed) for the transverse photocurrent.

where Δ denotes the effective broadening of the LL edge that cuts off the logarithmic divergence of the integral.

The sign and frequency dependence of the longitudinal distribution function contribution are determined by the function $-xB_1(x)$. This function is plotted in Fig. 4.7. We find negative photoconductivity in the frequency range $\omega < V_N$. For larger frequencies $V_N < \omega < 2V_N$, the sign of the photoconductivity changes. This sign change is a specific feature of our model, arising from the singular density of states at the band edge for the static periodic modulation potential. While this sign change is an interesting feature of our model and may be helpful in distinguishing between the displacement and the distribution function mechanism in an appropriate experiment, it is not expected to occur in a more generic situation, e.g. for disorder-broadened LLs, without a singularity at the Landau level edge. Specifically, for the case of disorder-broadened Landau levels relevant to current experiments, one expects a negative photoconductivity for all

$$\omega < 2V_N \quad . \tag{4.115}$$

Up to numerical factors, the result for the longitudinal distribution function photoconductivity, Eq. (4.112), differs from the corresponding result for *inter*-LL transitions [57] in two ways: the detuning $\Delta\omega = \omega_c - \omega$ is replaced by $-\omega$, and there is an additional prefactor $\beta\omega\nu_N(1-\nu_N)$. The first difference directly reflects the fact that initial, final, and intermediate states are *all* in the same Landau level. The additional prefactor stems from the difference in the thermal populations of initial and final state (which was equal to unity for *inter*-LL transitions). This provides a universal prescription to relate our results for the *intra*-LL photoconductivity to previous *inter*-LL results.

Displacement Mechanism

The DP contribution to the longitudinal photocurrent can be calculated from Eq. (4.51) using the equilibrium distribution function f^0_{nk} and the T-matrix contributions $T_\pm$.

In the limit $\omega \ll \omega_c$, only processes within the valence LL contribute to the photocurrent. Using Eq. (4.101) to express the difference between distribution functions in initial and final state, the longitudinal displacement photocurrent takes the form ($\sigma = \pm$)

$$\begin{aligned} j_x^{\mathrm{DP}} &= \frac{\pi e}{L_x L_y}\beta\omega\nu_N^*\left(1-\nu_N^*\right)\sum_\sigma\sum_{kk'}(k'-k)\ell_B^2 \\ &\quad\times\left|\langle Nk'\left|T_\sigma\right|Nk\rangle\right|^2\delta(\epsilon_{Nk}-\epsilon_{Nk'}+\sigma\omega) \quad . \end{aligned} \tag{4.116}$$

The real-space displacement between final and initial state due to disorder scattering is represented by $(k'-k)\ell_B^2$ in the above formula. Including the square of the transition matrix element given by Eq. (4.68) and performing the sum over k', we arrive at

$$\begin{aligned} j_x^{\mathrm{DP}} &= \frac{\pi e}{L_x L_y}\beta\omega\nu_N^*\left(1-\nu_N^*\right)\left(\frac{eE}{2\omega}\right)^2 \\ &\quad\times\quad\sum_\sigma\int\frac{d^2q}{(2\pi)^2}q_y\ell_B^2\left[q_y\ell_B^2 J_0(qR_c)\right]^2\tilde{W}(\mathbf{q}) \\ &\quad\times\quad\sum_k\delta(\epsilon_{Nk}-\epsilon_{Nk+q_y}+\sigma\omega) \quad . \end{aligned} \tag{4.117}$$

Using Eq. (4.38), the sum over k evaluates to

$$\begin{aligned} \sum_k\delta(\epsilon_{Nk}-\epsilon_{Nk+q_y}+\sigma\omega) &= \frac{L_xL_y}{2\pi V_N 2\pi\ell_B^2} \\ &\quad\times\quad\frac{1}{\sqrt{\sin^2\left(\frac{Qq_y\ell_B^2}{2}\right)-\left(\omega-eE_{dc}q_y\ell_B^2\right)}} \end{aligned} \tag{4.118}$$

so that the photocurrent assumes the form

$$\begin{aligned} j_x^{\mathrm{DP}} &= \frac{\pi e\beta\omega\nu_N^*\left(1-\nu_N^*\right)}{2\pi\ell_B^2 2\pi V_N}\left(\frac{eE}{2\omega}\right)^2 \\ &\times \sum_\sigma \sigma\int\frac{d^2q}{(2\pi)^2}\left(q_y\ell_B^2\right)^3\left[J_0(qR_c)\right]^2\tilde{W}(\mathbf{q}) \\ &\times \frac{1}{\sqrt{\sin^2\left(\frac{Qq_y\ell_B^2}{2}\right)-\left(\omega-eE_{dc}q_y\ell_B^2\right)}} \quad . \end{aligned} \tag{4.119}$$

The above expression contains a product of terms whose variations occur on different scales. While the Bessel function oscillates rapidly with q, the correlator $\tilde{W}(\mathbf{q})$ falls off at $q\sim\xi^{-1}\ll R_c/\ell_B^2=k_F$ and the square root term which stems from the k summation varies on the scale $q\sim a/\ell_B^2$. In the regime studied, $\lambda_F\ll a\ll\frac{\ell_B^2}{\xi}$, it is thus reasonable to separately average the latter and to factorize the $\mathbf{q}$-integration in the following way

$$\begin{aligned} j_x^{\mathrm{DP}} &= \frac{\pi e\beta\omega\nu_N^*\left(1-\nu_N^*\right)}{2\pi\ell_B^2 2\pi V_N}\left(\frac{eE}{2\omega}\right)^2 \\ &\times \sum_\sigma \sigma\int\frac{d^2q}{(2\pi)^2}\left(q_y\ell_B^2\right)^3\left[J_0(qR_c)\right]^2\tilde{W}(\mathbf{q}) \\ &\times \left\langle\left[\sin^2\left(\frac{Qq_y\ell_B^2}{2}\right)-\left(\omega-eE_{dc}q_y\ell_B^2\right)\right]^{-1/2}\right\rangle_{q_y} \quad , \end{aligned} \tag{4.120}$$

where $\langle\cdot\rangle_{q_y}$ indicates a separate averaging of the square root term over q_y. Keeping this term only to linear order in E_{dc} and introducing

$$x=\frac{\omega}{2V_N} \quad , \tag{4.121}$$

we find

$$\begin{aligned} \left\langle\left[\sin^2\left(\frac{Qq_y\ell_B^2}{2}\right)-\left(\omega-eE_{dc}q_y\ell_B^2\right)\right]^{-1/2}\right\rangle_{q_y} &= -\sigma\frac{eE_{dc}q_y\ell_B^2}{2V_N} \\ &\times \left\langle\left[\sin^2\left(\frac{Qq_y\ell_B^2}{2}\right)-x^2\right]^{-1/2}\right\rangle_{q_y} \quad . \end{aligned} \tag{4.122}$$

Finally performing the remaining $\mathbf{q}$-integration and expressing our result in terms of scattering times, we obtain

$$\sigma_{xx}^{\mathrm{DP}} \propto -\beta\omega\nu_N^*(1-\nu_N^*)\left(e^2\frac{R_c^2}{2\tau_{\mathrm{tr}}^*}\nu^*\right)\left(\frac{eER_c}{2\omega}\right)^2\frac{\tau_{\mathrm{s}}}{\tau_{\mathrm{tr}}^*}A_1\left(\frac{\omega}{2V_N}\right) \tag{4.123}$$

for the longitudinal displacement photoconductivity. The above relation contains a nonuniversal proportionality factor which depends on details of the smooth-disorder model.

One observes that this result is parametrically smaller than the distribution-function mechanism by a factor $\tau_s^*/\tau_{\rm in}$, where τ_s^* denotes the single-particle scattering time in the presence of the magnetic field. The function A_1 appearing in Eq. (4.123) is given by

$$\begin{aligned} A_1(x) &= -\frac{3}{2\pi}\frac{\partial}{\partial x}\frac{\ell_B^2}{a}\int_{-a/2\ell_B^2}^{a/2\ell_B^2} dq_y \frac{1}{\sqrt{\sin^2(Qq_y\ell_B^2/2)-x^2}} \\ &= -\frac{3}{\pi^2}\frac{\partial}{\partial x}K\left(\sqrt{1-x^2}\right) \end{aligned} \tag{4.124}$$

and is plotted in Fig. 4.7. Here, $K(x)$ denotes a complete elliptic function [76].

4.5.2 Transverse Photocurrent

We now turn to the calculation of the contributions to the transverse photocurrent. It was shown in Ref. [57] that within our model, the contributions of the displacement and the distribution-function mechanisms to the transverse photocurrent can be of the same order of magnitude for *inter*-LL transitions. We find the same conclusion to hold for *intra*-LL transitions, as will be shown below. We start by calculating the DF contribution to the transverse photocurrent.

Distribution Function Mechanism

The methods used in Ref. [57] can be readily extended to intra-LL transitions. As already discussed in Section 4.4.2, the essential new ingredient in computing the distribution-function contribution is a drift term $-eE_{dc}\partial f_{nk}/\partial k$ which enters the right-hand side of the kinetic equation Eq. (4.55), so that it takes the form given in Eq. (4.86). The transverse DF photoconductivity can be expressed as a function of the single-particle time in the presence of a magnetic field via

$$\sigma_{yy} = -\frac{e^2}{L_xL_y}\sum_k \left(\frac{\partial\epsilon_{Nk}^0}{\partial k}\right)^2 \tau_s^*(\epsilon_{Nk}^0)\frac{\partial\delta f_{Nk}^0}{\partial\epsilon_{Nk}^0} \quad . \tag{4.125}$$

The change in the distribution function is calculated from the kinetic equation. Finally, we arrive at the following result for the transverse distribution-function photoconductivity

$$\begin{aligned} \sigma_{yy}^{\rm DF} &= -4\,\beta\omega\,\nu_N^*(1-\nu_N^*)\left[e^2(v_y^2\tau_{\rm s}^*)\tilde{\nu}^*\right]\left(\frac{eER_c}{2\omega}\right)^2\frac{\tau_{\rm in}}{\tau_{\rm tr}^*} \\ &\quad\times B_2\left(\frac{\omega}{2V_N}\right) \quad , \end{aligned} \tag{4.126}$$

where B_2 is given by

$$B_2\left(\frac{\omega}{2V_N}\right) = -\frac{\partial}{\partial\omega}\int_{-V}^{V-\omega} d\epsilon \frac{1}{[\tilde{\nu}^*(\epsilon)]^2}\tilde{\nu}^*(\epsilon+\omega) \quad . \tag{4.127}$$

We obtain for this integral

$$B_2(x) = \left\{4x\left[\arcsin(1-2x)+\frac{\pi}{2}\right] - 4\sqrt{x-x^2}\right\} \quad . \tag{4.128}$$

The frequency dependence of the distribution function contribution is governed by the function $-xB_2(x)$. A plot of the implied frequency dependence is provided in Fig. 4.7.

Displacement Mechanism

Computing the displacement contribution to the transverse photoconductivity requires us to evaluate transition rates between quantum states corresponding to the "meander" equipotential lines in the presence of both static periodic modulation and dc electric field. Following the formalism developed in Ref. [57], we obtain

$$\begin{aligned}\sigma_{yy}^{\mathrm{DP}} &= -2\,\beta\omega\,\nu_N^*(1-\nu_N^*)\left[e^2(v_y^2\tau_{\mathrm{s}}^*)\tilde{\nu}^*\right]\left(\frac{eER_c}{2\omega}\right)^2\frac{\tau_{\mathrm{in}}}{\tau_{\mathrm{tr}}^*} \\ &\times \quad A_2\left(\frac{\omega}{2V_N}\right)\left(\frac{E_{\mathrm{dc}}^*}{E_{\mathrm{dc}}}\right)^2 . \end{aligned} \tag{4.129}$$

The frequency dependence of the photocurrent is described by the function

$$\begin{aligned}A_2(x) &= \frac{\pi\ell_B^2}{a}\int_{-a/2\ell_B^2}^{a/2\ell_B^2} dq_y \frac{x}{\sqrt{\sin^2(Qq_y\ell_B^2/2)-x^2}} \\ &= 2xK(\sqrt{1-x^2}) \quad . \end{aligned} \tag{4.130}$$

A plot of the frequency dependence implied by the function A_2 is provided in Fig. 4.7.

The transverse photoconductivity depends on the dc electric field E_{dc} in a singular way. This singularity is cut off for small dc electric fields by inelastic processes when

$$E_{\mathrm{dc}} \sim E_{\mathrm{dc}}^* \quad , \tag{4.131}$$

where [57]

$$E_{\mathrm{dc}}^* = Ba/2\pi\sqrt{\tau_{\mathrm{in}}\tau_s^*} \quad . \tag{4.132}$$

For

$$E_{\mathrm{dc}} \ll E_{\mathrm{dc}}^* \quad , \tag{4.133}$$

the photoconductivity crosses over to Ohmic behavior, matching with Eq. (4.129) for

$$E_{\mathrm{dc}} \sim E_{\mathrm{dc}}^* \quad . \tag{4.134}$$

This implies that the contributions by displacement and distribution mechanisms are of the same order of magnitude in the transverse case.

4.6 Comparison with Experiment

Strictly speaking, our model deviates from the experimental system, due to the assumption of a static periodic modulation potential and the neglect of disorder broadening of the Landau bands. However, previous work [57] shows that

the magnitude of the longitudinal photocurrent obtained within our model is parametrically identical to that for disorder-broadened Landau levels when one identifies modulation broadening with disorder broadening. Specific features arise within our model due to its anomalous density of states at the LL edge (see Fig. 4.4), leading to additional sign changes of the photocurrent. These artefacts would not be present in a thorough microscopical treatment of disorder. Their advantage, in turn, is that the differences in the behavior of DP and DF contributions within our model might help to discern between the two mechanisms in experiment.

Keeping these caveats in mind, the results obtained within our model can be compared to the experiment of Ref. [39]. It turns out that our model is indeed capable of describing the key experimental observations. Our main results relevant to experiment are:

(i) When ignoring effects of the singular density of states at the LL edge – which are due to our specific model – the sign of the photocurrent due to intra-LL transitions is negative, leading to a reduction of the experimentally observed resistivity.

(ii) Comparing the longitudinal photoconductivity in Eq. (4.112) to the dark conductivity $\sigma_{xx}^{\mathrm{dark}} = e^2(R_c^2/2\tau_{\mathrm{tr}}^*)\nu^*(\Gamma/T)$, we find that their ratio depends on magnetic field as $\sigma_{xx}^{\mathrm{DF}}/\sigma_{xx}^{\mathrm{dark}} \sim R_c^2/\Gamma\tau_{\mathrm{tr}}^* \sim 1/B^2$ at fixed ω. This magnetic-field dependence actually also holds for inter-LL processes [57]. Here, we used that for both disorder-broadened LLs as well as modulation-broadened LLs, the LL broadening Γ scales with magnetic field as $\Gamma \sim \sqrt{B}$.

(iii) The amplitude of the photoconductivity due to intra-LL transitions scales as $1/\omega$ with the microwave frequency, see Eq. (4.112).

(iv) Due to the factor $\nu_N^*(1-\nu_N^*)$, the magnitude of the effect is strongest for half-filled LLs and falls off to zero when the valence LL is either empty or completely occupied. We note that this filling-factor dependence is specific to intra-LL transitions and does not occur for inter-LL transitions near the cyclotron resonance or its harmonics [57].

These results are in good agreement with the key experimental observations: (i) explains the sign of the effect. In experiment, there is indeed a considerable reduction of the resistivity in the regime $\omega \ll \omega_c$ due to irradiation with microwaves. (ii) is in agreement with the observation that over the magnetic-field range where intra-LL processes dominate, the relative microwave-induced suppression of the conductivity decreases as the magnetic field increases (see Fig. 1 of Ref. [39]). In addition, this magnetic-field scaling explains why, experimentally, it is apparently harder to reach zero-resistance in the regime of intra-LL transitions which occur at higher magnetic fields compared to the cyclotron resonance or its harmonics. (iii) is in accordance with the observation that the microwave-induced reduction of the diagonal resistivity decreases with increasing microwave frequency (see Fig. 2 of Ref. [39]). Finally, (iv) implies

that the photoconductivity suppresses the Shubnikov-deHaas oscillations, an effect which was very pronounced experimentally.

4.7 Polarization Dependence

The results presented so far are only valid for microwaves polarized linearly in the x-direction. In this section, we expand our considerations to microwaves polarized linearly in the y-direction or polarized linearly in an arbitrary direction and to microwaves of circular polarization. We recall that in the *inter*-LL case, there was no polarization dependence in the former, but a strong polarization dependence in the latter case, where, depending on the sign of the circular polarization, either no photoconductivity or double the photoconductivity of the linearly polarized case was recorded [57].

In the *intra*-LL case, it turns out that for microwaves polarized linearly in the y-direction or any other direction, only the subdominant displacement contribution to the longitudinal photoconductivity exhibits a polarization dependence, while all other contributions are polarization-independent. For circularly polarized microwaves, the magnitude of the displacement contribution to the longitudinal photoconductivity changes with respect to linearly polarized microwaves, but there is no dependence on the type of circular polarization. Both displacement and distribution-function contribution to the *intra*-LL transverse photocurrent are independent of the type of polarization.

These results for the polarization dependence will now be derived. If the microwaves are polarized linearly in y-direction, they can be described by the potential

$$\tilde{\phi}(\mathbf{r},t) = -eEy\cos(\omega t) = \tilde{\phi}_+ e^{-i\omega t} + \tilde{\phi}_- e^{i\omega t} \quad . \tag{4.135}$$

The corresponding matrix elements between the LL states in the Landau gauge for intra-LL-processes are then given by

$$\langle nk'|\tilde{\phi}_\pm|nk\rangle = -\frac{eE}{2}\left[\frac{1}{i}\frac{\partial}{\partial k}\delta(k'-k)\right] e^{-(k-k')^2\ell_B^2/4} L_n^0\left(\frac{(k'-k^2)\ell_B^2}{2}\right) \quad . \tag{4.136}$$

Using these microwave matrix elements and again neglecting subdominant contributions from processes with intermediate states outside of the valence LL, a calculation analogous to that presented in Section 4.5.1 yields for the displacement photoconductivity in the direction of modulation

$$\tilde{\sigma}_{xx}^{DP} = \frac{1}{3}\,\sigma_{xx}^{DP} \quad , \tag{4.137}$$

expressed as a function of the result for microwaves polarized in x-direction, σ_{xx}^{DP}. For microwaves polarized linearly in y-direction, the displacement contribution to the longitudinal photoconductivity thus is only one third of the prior result for microwaves polarized linearly in x-direction.

The other photoconductivities for microwaves polarized in y-direction are calculated in a similar way and turn out to be unaltered from the prior results for microwaves polarized linearly in x-direction, i.e.

$$\tilde{\sigma}_{xx}^{DF} = \sigma_{xx}^{DF} \quad , \quad \tilde{\sigma}_{yy}^{DF} = \sigma_{yy}^{DF} \quad , \quad \tilde{\sigma}_{yy}^{DP} = \sigma_{yy}^{DP} \quad . \tag{4.138}$$

The photoconductivity along the direction of modulation thus depends on the specific type of linear polarization. This dependence, however, is weak since the dominant contribution from the distribution function mechanism turns out to be polarization-independent. For the photoconductivity in the y-direction, where in principle the contributions of displacement and distribution function mechanisms are of the same order, there is no polarization dependence.

For a general, linearly polarized microwave field, we thus expect a weak polarization dependence of the longitudinal photoconductivity. Using

$$\phi_{lin} = \frac{e}{2}(xE_x + yE_y)\cos(\omega t) \quad , \tag{4.139}$$

one finds

$$\sigma^{DP}_{xx,lin} = \left(\frac{E_x^2}{E_x^2+E_y^2} + \frac{1}{3}\frac{E_y^2}{E_x^2+E_y^2}\right)\sigma^{DP}_{xx} \quad , \tag{4.140}$$

while all other contributions are polarization-independent.

Finally, we address the case of circular polarization. As was noted in passing above, prior work for *inter*-LL transitions [57] demonstrated a strong dependence on the sign of the circular polarization in the vicinity of $\omega = \omega_c$. The physical reason for this consists of a strong rectification of the cyclotron radiation in the co- and contragredient cases, leading to an extinction of the photoconductivity or to an increase by a factor of two. Here, we are interested in the case $\omega \ll \omega_c$, with a microwave frequency ω far from resonance. We therefore do not expect such drastic effects on the photoconductivity. Using

$$\hat{\phi}_{\sigma\pm} = -\frac{eE}{\sqrt{2}}\left[x\cos(\omega t) \pm y\sin(\omega t)\right] \quad , \tag{4.141}$$

where $\sigma\pm$ denotes the sign of the circular polarization, we find (σ^{DP}_{xx} is the displacement contribution to the longitudinal photoconductivity for microwaves polarized linearly in x-direction)

$$\hat{\sigma}^{DP}_{xx,\sigma+} = \hat{\sigma}^{DP}_{xx,\sigma-} = \frac{2}{3}\sigma^{DP}_{xx} \tag{4.142}$$

and no change (with respect to linearly polarized microwaves) for all other contributions. It is interesting to note that in the case studied, there is no dependence on the sign of the circular polarization. This is markedly different from the *inter*-LL case.

4.8 Discussion

In this chapter, we studied the microwave photoconductivity of a 2DEG in a perpendicular magnetic field with an additional unidirectional static periodic modulation in the regime of intra-LL transitions. We identified the dominant disorder-assisted microwave absorption and emission processes within this regime and computed both the longitudinal and transverse photocurrents.

We find that the distribution-function mechanism dominates for the longitudinal photocurrent while both distribution-function and displacement mechanism contribute to the same order to the transverse photocurrent. Except for

subdominant contributions, we find that the photoconductivity due to intra-LL processes is polarization-independent. The singular density of states of our model near the LL edges leads to interesting sign changes, rendering the photoconductivity positive within certain frequency ranges. With the exception of these model-specific predictions, our results are in excellent qualitative agreement with experiment. Specifically, we are able to explain the microwave-induced suppression of the Shubnikov-deHaas oscillations in the regime of intra-LL transitions.